Identification and relative quantification of 3-nitrotyrosine residues in fibrinogen nitrated *in vitro* and fibrinogen from ischemic stroke patient plasma using LC-MS/MS.

Romina Medeiros[1]; Bebiana Sousa[2]; Silvina Rossi[1]; Catarina Afonso[2]; Luis Bonino[1]; Andrew R. Pitt[2,3]; Elizabeth López[1]; Corinne M. Spickett[2]; Graciela Borthagaray[1]

[1]Facultad de Química, Universidad de la República, Montevideo, Uruguay

[2]School of Life and Health Sciences, Aston University, Birmingham, UK.

[3] Manchester Institute of Biotechnology, University of Manchester, 131 Princess Street, Manchester. M1 7DN, UK

Corresponding Author: Romina Medeiros, Facultad de Química, Universidad de la República, Montevideo, Uruguay. Email: rominamedeiros7@gmail.com

Abstract

Ischemic stroke is one of the leading causes of death and disability worldwide. This acute vascular event interferes with blood supply to the brain and induces a burst of free radicals such as nitric oxide and superoxide, producing peroxynitrite, a precursor of strong nitrating agents. Fibrinogen is one of the most abundant plasma proteins; it plays a role in the hemostatic system, mediating clot formation, which can be affected by nitrotyrosine formation. We hypothesized that nitration of fibrinogen by ONOOH and $ONOOCO_2^-$ radical products could be one of the early events of the ischemic stroke, and protein-bound 3-nitrotyrosine could be a potential biomarker for diagnosis and/or prognosis of this condition. A targeted mass spectrometry approach was developed to analyze the nitration of fibrinogen and its association with ischemic stroke. First, a comprehensive mapping of 3-nitrotyrosine locations and their relative quantification was performed by LC-MS/MS, using *in vitro* nitrated fibrinogen samples. Twenty different 3-nitrotyrosine residues were identified on fibrinogen nitrated *in vitro*, varying with the peroxynitrite: fibrinogen molar ratio used. Nine tyrosine residues that were consistently modified at different treatment ratios were chosen to perform a targeted LC-MS/MS analysis in clinical samples. Enriched fibrinogen fractions from clinical samples from 24 ischemic stroke and 12 patients with non-inflammatory conditions were analyzed with this method. Three of the nine tyrosine residues analyzed (βY452, βY475 and γY380) showed a significant difference between the ischemic stroke and non-inflammatory disease groups. ROC curve analysis suggested an association of these residues either individually or in combination with ischemic stroke. Different tyrosine nitration patterns were also observed in fibrinogen modified *in vitro* and *in vivo*, suggesting differences in the nitration process in these situations. This is the first study showing a putative association between the nitration profile of specific tyrosine residues in human fibrinogen and ischemic stroke.

Keywords

Nitroxidative stress; tandem mass spectrometry; inflammation; oxidative post-translational modification; biomarkers; diagnostic methods; ROC curve analysis

1. Introduction

Stroke is the major cause of long-term adult disability and one of the leading causes of death worldwide [1, 2]. Broadly speaking, there are two types of stroke, either ischemic stroke, which accounts for approximately 85 % of cases, or hemorrhagic stroke, which occurs in 15 % of cases. Ischemic stroke is an acute vascular event that interferes with blood supply to the brain due to the obstruction of a cerebral blood vessel by a clot [3]. The current treatment is clot lysis with recombinant tissue plasminogen activator (rtPA); however, due to its narrow therapeutic time window, less than 5 % of stroke patients are able to receive it [4, 5]. Therefore, tools for earlier and accurate diagnosis of ischemic stroke, which would reduce mortality, neurological deficits and systemic damage associated with late diagnosis are highly desirable, as well as a better understanding of stroke pathology [6].

During the acute cerebral ischemia caused by the lack of blood supply, nitric oxide ($^{\bullet}NO$), a free radical species, is increasingly released in order to protect the cerebral parenchyma by promoting vasodilation and improving reperfusion [7, 8]. Reperfusion also induces a burst of other free radicals including superoxide ($O_2^{\bullet-}$), which can react in a diffusion-controlled manner with $^{\bullet}NO$ to produce the reactive, short-lived anion peroxynitrite ($ONOO^-$) [9]. The protonated species peroxynitrous acid (ONOOH) is a good oxidant and nitrating agent, which can generate the secondary free radical products $^{\bullet}NO_2$ and $^{\bullet}OH$. In the presence of CO_2 it can also produce the peroxynitrosocarbonate anion ($ONOOCO_2^-$), which homolyzes to $^{\bullet}NO_2$ and $CO_3^{\bullet-}$ radicals. These secondary products have been shown *in vitro* to be important in the nitration of tyrosine at the ortho position of the phenolic ring to form 3-nitrotyrosine, which is enhanced in the presence of CO_2 or bicarbonate buffers [10-12]. Current understanding of the reactions of peroxynitrite and biochemical effects of its downstream products have been thoroughly

reviewed recently by Ferrer-Sueta et al. [13]. Thus, ischemic conditions in the brain trigger nitroxidative stress through the generation of peroxynitrite, which has also been shown to alter the permeability of the blood brain barrier [14]. Peroxynitrite derivates can lead to harmful effects on circulating plasma proteins due to their high reactivity, half-life of 1-2 seconds and action radius of around 100 µm [15], which allows them to reach the lumen of blood vessels. *In vivo*, the nonenzymatic nitration of protein tyrosine residues is a recognized oxidative post-translational modification (oxPTM) with important pathophysiological consequences [16]. It can cause alterations in protein structure and function [17], and therefore the formation of peroxynitrite and 3-nitrotyrosine in the cardiovascular system could lead to dysfunction of important plasma proteins.

Fibrinogen is the third most abundant plasma protein (approx. 4 % of total plasma protein), and plays a central role in the hemostatic system, a physiological process related to stroke development, mediating clot formation by its aggregation as fibrin monomers to form an insoluble polymer [18]. A direct relationship between stroke and high levels of fibrinogen has been previously reported, both as a risk factor and a poor prognosis factor [19]. Studies of fibrinogen *in vitro* have demonstrated that fibrinogen is highly susceptible to oxidant attack, including nitration by peroxynitrite products, and investigations of the differential susceptibility of plasma proteins to nitroxidative modifications indicated that the same is true in a physiological environment [20]. Nitrated fibrinogen has been found in a variety of stress and pathological conditions. For example, the process of ageing has been associated with the production of nitroxidative agents and the presence of nitrated fibrinogen, among other modified proteins [21]. Parastatidis *et al*. found nitrated fibrinogen peptides in plasma samples from smokers using a tandem mass spectrometry approach [22]. Oxidative stress in diabetic patients with atherosclerotic complications has been shown to lead to intravascular fibrous deposits that were found to contain oxidized fibrin(ogen)-like material, in addition to oxidized LDL, as reviewed by Lipinski [23]. Nitrated fibrinogen has been reported as a potential biomarker

for coronary artery disease, with an increase of its levels being measured in plasma, as well as functional alterations in the physical properties of fibrinogen/fibrin leading to a pro-thrombotic state [24]. Other diseases such as acute respiratory distress syndrome [25], lung cancer [26], end-stage renal disease [27] and venous thromboembolism [28] have also been associated with the presence of oxidized and nitrated fibrinogen. The nitration of fibrinogen by peroxynitrite derivatives and its potential role in ischemic stroke have been reported once before: Ill-Raga *et al.* found that ischemic conditions induced nitroxidative stress and fibrinogen nitration, which influenced its structure and hemostatic properties, as well as causing damage to the neuronal parenchyma [29]. In order to obtain a better understanding of the biological effects of fibrinogen tyrosine nitration in diseases, a comprehensive analysis of the sites of modification is required.

The mapping of sites of nitration of fibrinogen is challenging work, as fibrinogen is a complex protein composed of pairs of three different polypeptide chains: α, β (also called Aα and Bβ, to denote that each chain contains the sequences corresponding to fibrinopeptides A and B, respectively) and γ [30]. Moreover, the numbers of tyrosine residues differ between different isoforms of the chains. The fibrinogen α gene is spliced into two alternative isoforms, 1 and 2. The isoform 2 is shorter, lacking the C-terminal fibrinogen-like domain of isoform 1, and it largely predominates over isoform 1. The α chain isoforms differ significantly in tyrosine content: isoform 1 has 24 tyrosine residues and is present in fibrinogen with a molecular mass of 420 kDa, which only accounts for about 2% of fibrinogen in the whole pool, whereas isoform 2 has only 9 tyrosine residues and is present in fibrinogen with a molecular mass of 340 kDa, constituting 98% of human plasma fibrinogen [31]. The γ gene is spliced into gamma-A or gamma-B isoforms. Mature forms of gamma-A and gamma-B chains have 20 and 22 tyrosine residues respectively, and gamma-A predominates over gamma-B in humans. Two additional tyrosine residues are present in the gamma chain signal peptide, which is removed before fibrinogen is assembled in the hepatocyte [32]. In contrast, the β chain has only one known isoform in humans, which contains 21 tyrosine residues [30].

It is possible to study which chains in peroxynitrite-modified fibrinogen contain 3-nitrotyrosine residues by Western blotting, but for specific identification and localization of modified residues liquid chromatography coupled with tandem mass spectrometry is required. Analyzing fibrinogen nitrated *in vitro* using peroxynitrite, Tang *et al.* identified 26 different 3-nitrotyrosine sites across the three fibrinogen subunits, among a total of 39 tyrosine residues that were observed in the experiments [33]. Luo *et al.* found that fibrinogen polypeptide γ chain was nitrated in a concentration-dependent manner on exposure to peroxynitrite [34]. Analysis of the γ chain determined that the extent of nitration of the identified 3-nitrotyrosine sites was directly proportional to the ratio $ONOO^-$ to protein used, and overall, five susceptible nitration sites on that chain were identified. A recent analysis of $ONOO^-$-treated fibrinogen indicated that the amount of 3-nitrotyrosine increased with $ONOO^-$ concentration in a dose-dependent manner, and that the chains show a different susceptibility, but in contrast to previous work the α chain was found to be the most susceptible, not only to nitration but also to oxidation [35]. Oxidation of fibrinogen with two concentrations of SIN-1, a peroxynitrite generator, resulted in a range of modifications in all chains, predominantly methionine sulfoxide and nitrotyrosine, the amount of which correlated with increasing SIN-1 treatment [36]. Thus, there remains some variability in the modifications detected in different studies, and more work to develop methodology is needed for translation to functional and diagnostic studies.

These studies suggest that modified fibrinogen has potential as a biomarker that could help the diagnosis and prognosis of diseases with a nitroxidative etiology, such as ischemic stroke, but as yet there has been no comprehensive analysis of the sites of nitration in this condition. We therefore developed a mass spectrometry approach to detect and quantify the nitration of fibrinogen and assess the nitration of specific residues in ischemic stroke. In the first stage of the work, fibrinogen was modified *in vitro* using 3 different concentrations of peroxynitrite, and the modifications were extensively mapped by an untargeted LC-MS/MS approach to identify the most susceptible residues. Subsequently, a targeted multiple reaction monitoring (MRM)

method, as well as a corresponding selected reaction monitoring (SRM) method to improve overall sensitivity, was set up for the relative quantification of the most susceptible residues, and tested by investigation of 3-nitrotyrosine formation in plasma fibrinogen from ischemic stroke patients.

2. Materials and Methods

2.1. Chemicals

All reagents were obtained from Sigma-Aldrich, unless otherwise specified, and were of Analar® quality or better. All solvents were of LC-MS/MS grade and all solutions were prepared with ultra-pure Type 1 water.

2.2. Plasma from healthy volunteer subjects

Blood from five healthy volunteers (mean age of 30 years) was taken with informed consent by venipuncture into EDTA vacutainers. Plasma was obtained by centrifugation at 2500 g for 10 minutes, subsequently pooled and stored in aliquots at -80°C. Volunteers were without risk factors for thrombotic or cardiovascular events, and had no other relevant diseases. The protocol was approved by the Research Ethics Committee of Aston University.

2.3. Fibrinogen

PEG-isolated human fibrinogen [37] from healthy donors' plasma and a commercial preparation from Sigma-Aldrich were used as a source of fibrinogen for peroxynitrite treatments *in vitro* and as the untreated control.

2.4. *In vitro* nitration of fibrinogen and healthy donors' plasma

PEG-isolated human fibrinogen was nitrated *in vitro*, using peroxynitrite synthesized in-house, at a range of molar equivalents. Peroxynitrite was synthesized as described by Beckman *et al*. [38]. Briefly, hydrogen peroxide was added to a sodium nitrite solution in a flask cooled to 0°C in an ice bath, with continuous stirring, followed by the rapid addition of hydrochloric acid, and then sodium hydroxide to stop the reaction. Excess hydrogen peroxide was quenched by the

addition of solid manganese dioxide followed by filtration to remove the solid. The concentration of peroxynitrite was determined by the increase in absorbance at 302 nm (ε_{302nm}= 1.670 $M^{-1}cm^{-1}$) in 1.2 N NaOH.

Human fibrinogen (4 mg/mL) was nitrated with the chemically synthesized peroxynitrite in 100 mM potassium phosphate, 25 mM sodium bicarbonate, 100 μM diethylene triamine pentaacetic acid (DTPA), pH 7.4. A small volume (less than 1% of total reaction volume) of peroxynitrite solution was added to a tube containing the fibrinogen solution, followed immediately by vigorous vortexing [35]. As bicarbonate buffer was used, it is likely that the peroxynitrosocarbonate ($ONOOCO_2^-$) anion was formed, leading to enhancement of tyrosine nitration. To obtain fibrinogen with different degrees of nitration, three different molar ratios of peroxynitrite to fibrinogen were used: 200, 100 and 10 moles of $ONOO^-$ per mole of fibrinogen. The 3-nitrotyrosine concentration in each case was determined by measuring the absorbance of an alkaline solution of the nitrated fibrinogen (pH ≥ 9) at 420 nm (ε_{420nm}=4300 $M^{-1}cm^{-1}$) and the fibrinogen concentration was determined by measuring the absorbance of a neutral solution (pH = 7) at 280 nm (ε_{280nm}=5.14 x 10^5 $M^{-1}cm^{-1}$). Finally, the 3-nitrotyrosine content of nitrated fibrinogen was estimated as the molar ratio of 3-nitrotyrosine to protein. Nitrated fibrinogen preparations were dialysed against 0.02 M sodium citrate, 0.15 M NaCl, pH 7.4, with PMSF 1 mM and 0.2 g/L sodium azide and stored at -80°C as stock solutions of 1 mg/mL. Additionally, plasma from a healthy donor pool was nitrated following the same procedure but using a ratio of 5 moles of $ONOO^-$ per mole of total protein.

The peroxynitrite-treated fibrinogen solutions were analysed by LC-MS/MS using IDA, MRM and SRM modes as described below. Plasma treated *ex vivo* with peroxynitrite, and a fibrinogen enriched fraction from it, were analysed by LC-MS/MS in MRM and SRM modes only.

2.5. Clinical Subjects

We performed an observational case-control study of consecutive subjects, 18 years of age or older, who arrived at the Hospital Maciel Emergency Department (Montevideo, Uruguay) with

suspected ischemic stroke. The exclusion criteria included hemorrhagic stroke and an inability to provide informed consent. Ischemic stroke was diagnosed by magnetic resonance imaging. A total of 24 patients with ischemic stroke was studied, with a mean of 70 years old (12 women and 12 men). Secondary variables were also collected, including demographic information, thrombotic risk factors and comorbidities, and these are shown in **Table 1**. Blood extraction was carried out during a window of 1 to 36 hours after the first symptoms of ischemic stroke and before initiation of anticoagulant therapy (if it was applicable). Patients presenting at the Emergency Department for non-cardiovascular-related conditions during the same period were included in the study as controls. Inclusion criteria for these patients were to belong to the same age group (18 to 85 years old), to present a low risk of future heart attack and stroke according to the American Heart Association (hsCRP lower than 1 mg/L [39]), and without risk factors or medical history of cardiovascular diseases, with a mean age of 49 years (8 women and 4 men) (Table 1). Blood was collected from patients in 3.2 % sodium citrate (BD Vacutainer; Franklin Lakes, NJ, USA), centrifuged at 2500 g for 10 minutes, and plasma samples were transferred to new tubes followed by storage at -80 °C for further analysis. All protocols were scrutinized and approved by the Ethics Committee of Facultad de Química at Universidad de la República, Hospital Maciel; written informed consent was obtained from all study participants.

2.6. Fibrinogen enrichment from ischemic stroke and control subjects for the LC-MS/MS analysis

Fibrinogen from patient plasma samples was enriched by glycine precipitation, as described previously [22]. The pellets obtained were reconstituted in the minimum volume of 50 mM Tris, 140 mM NaCl, pH 7.4 required to obtain complete dissolution (20-50 μL) for analysis by mass spectrometry.

2.7. Preparation of samples for MS analysis: in-solution digestion using RapiGest SF

Fibrinogen enriched fractions were digested in-solution with trypsin in presence of RapiGest SF surfactant (Waters, UK) following the manufacture´s recommended procedure. Briefly, 100 μL of 0.1 % RapiGest SF were added to 20 μL of fibrinogen solution (approx. 100 μg) and mixed

vigorously. Dithiothreitol (DTT) was added to each sample to give a final concentration of 5 mM, and incubated at 60°C for 30 minutes. Free cysteine residues were alkylated by the addition of iodoacetamide to a final concentration of 15 mM and incubated at room temperature in the dark for 30 minutes. Finally, MS grade trypsin (2.25 μg; Promega, Southampton, UK) was added and the samples were incubated at 37°C overnight. To prepare samples for LC-MS, 99% trifluoroacetic acid (TFA) was added to give a 1% final concentration and allowed to react for 30 minutes at 37°C. The acid-treated samples were then centrifuged at 10,000 g for 10 minutes at room temperature and the clarified supernatants transferred to a clean microcentrifuge tube and dried under vacuum. The pellets were reconstituted in 30 μL of eluent A (see below) and transferred into screw top auto-sampler glass vials (Chromacol, Speck and Burke Analytical, UK). The same protocol was followed for digestion of nitrated whole plasma.

2.8. Mass spectrometry on Information-Dependent Acquisition mode and spectra evaluation

Samples were analysed on a TripleTOF® 5600 System (SCIEX, UK) coupled with a Dionex Ultimate 3000 High Performance Liquid Chromatography system (Thermo Scientific, UK). The mobile phases consisted of solvent A (98 % H_2O, 2 % acetonitrile, 0.1% formic acid) and solvent B (98 % acetonitrile, 2 % H_2O, 0.1 % formic acid). The peptide solution was loaded onto a C18 trap column (C18 PepMap™, 5 μm, 0.5 x 5 mm, Thermo Scientific, Hemel Hempstead, UK) using solvent A at 20 μL/min before separation on a nano-HPLC column (C18 PepMap™, 5 μm, 0.075 x 150 mm, Thermo Scientific, Hemel Hempstead, UK). For separation, the flow rate was 0.3 μL/min, with a gradient elution running from 2 % to 45 % solvent B over 45 minutes, followed by ramping to 90 % solvent B in 1 minute. The gradient was held at 90 % solvent B for 5 minutes and then re-equilibrated to the starting solvent for 5 minutes. The total time per chromatographic run was approximately 1 h. Peptides eluted from the column were ionized with a spray voltage of 2.4 kV, a source temperature of 150 °C, a de-clustering potential of 50 V and a curtain gas setting of 15. Survey scans were collected in positive ion mode in a range of 350 to 1250 Da for 250 ms using the high resolution TOF-MS mode. Information-Dependent Acquisition

(IDA) was used to collect MS/MS data using the following criteria: the 15 most intense ions with 2+ to 5+ charge states and a minimum intensity of 500 counts per second (cps) using dynamic exclusion for 30 s, 100 ms acquisition and a fixed collision energy setting of 50 ± 15 V. The peak areas in the extracted ion chromatograms (XICs) of the parent peptides were integrated by PeakView® and the percentage nitration of the peptide was calculated using the following equation: Nitrated peptide (%) $= \frac{\text{Peak Area nitrated peptide}}{\text{Peak Area nitrated peptide + Peak Area native peptide}} \times 100.$

2.9. Database Searches

The Mascot search engine (Matrix Science, UK, version 2.4.0) was used to interrogate the *Mammalia* taxonomy section of the SwissProt database (2018_08). This database contains isoform 1 of the α chain (long isoform), the β chain, and isoform B (including the signal peptide) of the γ chain of human fibrinogen. Searches were performed on raw .wiff files using the Mascot search engine with SCIEX data converter, with variable modifications of nitration of tyrosine and tryptophan (+45 Da), amination of tyrosine (3-aminotyrosine, +15 Da), oxidation of methionine, tyrosine and tryptophan (+16 Da), trioxidation of cysteine (+48), kynurenin formation from tryptophan (+ 4Da), deamidation of asparagine and glutamine (+ 1 Da), and carbamidomethyl-cysteine (+57 Da). The latter was searched as a variable modification because nitroxidative treatments may cause irreversible modifications of cysteine that prevent reaction with iodoacetamide. The protease selected was trypsin, with a maximum of 2 missed cleavages. The search was set to identify peptides by their monoisotopic masses, with 2+, 3+ and 4+ charge states. The MS and MS/MS tolerance were set to ± 0.6 Da. Peptides identified by Mascot were validated by *de novo* sequencing of the MS/MS data using PeakView® analysis software, version 2.2 (SCIEX, UK).

2.10. Mass spectrometry: Multiple Reaction Monitoring (MRM) and Selected Reaction Monitoring (SRM)

For the analysis of clinical samples, MS experiments were carried out in triplicate. Peptides were separated and analysed using an Ultimate 3000 system (Thermo Scientific, Hemel Hempstead,

UK) coupled to a QTrap® 5500 (SCIEX, Warrington, UK). The solvent system was as described above. The peptide solution was loaded directly onto a C18 column (C18 PepMap™ 100, 5 µm, 300 µm x 25 cm, Thermo Scientific, Hemel Hempstead, UK) at 5 µL/min, and eluted using a gradient elution running from 2 % to 45 % solvent B over 45 minutes. Ionization of the peptides was achieved with a spray voltage set at 5.5 kV, a source temperature of 150 ^{o}C, declustering potential of 70 V. Analysis was carried out in MRM scanning mode. The total scan time was 0.7 seconds, dwell time ranged between 20 and 70 ms depending on the transitions and collision energies were calculated for all transitions and set at the second quadrupole using b or y series ions. The transitions were developed based on the modified peptides identified in the previous analyses. Peaks were considered quantifiable if the signal to noise ratio was ≥8. The percentage nitration of the peptide was calculated as explained in section 2.8.

2.11. Statistics

Statistical analysis was performed using SPSS Statistics software. Gaussian probability distribution of the data set for each clinical cohort was assessed using a Kolmogorov-Smirnov test. When the K-S test rejected the Gaussian distribution hypothesis, the non-parametric Mann-Whitney U (M-W) test for two independent samples was used to compare clinical sample data.

3. Results

3.1. Characterization of *in vitro* nitrated fibrinogen peptides by LC-MS/MS

The occurrence of 3-nitrotyrosine was identified by ESI-QTOF MS analysis of fibrinogen nitrated *in vitro* and digested in-solution. Mascot was able to identify the α, β and γ chains of human fibrinogen with an average of 56%, 76% and 80% sequence coverage, respectively, and confirmed that the predominant isoform of α chain was 2 and of γ chain was A. The sequence coverage of the α chain was better than implied, as Mascot assumed the long isoforms for the α and γ chains. A number of 3-nitrotyrosine residues were identified by a 45 Da mass increase due to the addition of -NO_2 to tyrosine residues, with the corresponding loss of hydrogen. All

peptide ions containing this modification, and their corresponding unmodified peptides, were validated by *de novo* sequencing of the MSMS spectra, as shown for the unmodified and nitrated forms of peptide β^{472}GSWYSMR from the β-chain (**Figure 1A** and **B** respectively). **Figures 1C & D** show the extracted ion chromatograms (XICs) for the unmodified and modified peptide β^{472}GSWYSMR respectively, and it can be seen that in untreated fibrinogen only the native peptide was observed. The peak areas were used to calculate the % nitration for each peptide. No 3-nitrotyrosine modifications were identified by Mascot in untreated (native) fibrinogen samples under comparable search conditions, although the scores of unmodified peptides were similar to those in the nitrated samples.

Table 2 lists the nitrated peptides identified and validated for the three chains of *in vitro* nitrated fibrinogen (for all the nitroxidative treatments) and the 3-nitrotyrosine percentage for each peptide. Twenty different tyrosine nitration sites were identified across the three fibrinogen subunits out of the 50 tyrosine theoretically present within the predominant fibrinogen isoforms. The number of tyrosines and nitrotyrosines observed in each of the chains under different treatment ratios are shown in Supplementary table S1. Although 10 tyrosines in the alpha chain were observed, 9 were from the short isoform and the 10^{th} (from the C-terminal region of the long isoform) had only a single peptide incidence and the XIC had an intensity 1-2% of the other peptides, consistent with the expected level of this form in plasma. Overall, the highest treatment ratio gave more modifications and/or higher % levels of nitrotyrosine in the peptides compared to the lower treatment ratios, although there was not always a clear dose-dependence. Nitration at residues βY71, βY475 and γY389 were the most consistently identified, despite the fact that Y475 showed relatively low percentage modification. The XIC data for the untreated fibrinogen preparations typically showed intense peaks for the native peptide ions but no peaks for any of the modified peptides were observed, as shown for the example peptide β^{472}GSWYSMR in Figure 1.

The alpha chain appeared to be highly susceptible to peroxynitrite, as the 4 tyrosine residues that were nitrated at 200:1 molar ratio showed high percentage modification, and at 100:1 molar ratio nitration of 2 peptides was also observed. The beta chain also showed extensive modification at the highest treatment conditions, with 10 out of 21 peptides identified as modified, whereas only 6 out of 18 tyrosine-containing peptides were seen to be modified in the gamma chain, and only at the highest treatment ratio. For both the beta and gamma chains, the % nitration of the peptides were generally low except at the 200:1 molar ratio, where several tyrosine residues were 20-50 % nitrated.

A large number of peptides containing variable methionine oxidation were also observed in the Mascot searches. These were not validated or investigated further as this was not the focus of the study, although there is known to be a CO_2-dependent effect on methionine oxidation by peroxynitrite products (Berlett)). In contrast, the occurrence of other oxidations, including cysteine trioxidation and formation of hydroxy-tyrosine, amino-tyrosine, hydroytryptophan, kyneurenin and oxo-histidine was minimal. An oxidation of βW415 in peptide DNDGWLTSDPR (m/z 795.40 [2+]; R_t 22.6 mins) was identified only in the highest treatment concentration. Two nitrotryptophan-containing peptides were found in 200:1 $ONOO^-$: Fg treatment: βW470 in peptide HGTDDGVVWMNWK (m/z 795.40 [2+]; R_t 29.2 mins) at ~0.65% modification and βW474 occurred in dinitrated peptide GSWYSMR (m/z 488.71 [2+]; R_t 27.7 mins) at 4.4% only when the tyrosine was already modified, which might also be expected from the relative reactivities of the phenol and indole rings; a mono-nitration of W only was below the limit of detection. As the tryptophan nitrations were so uncommon and occurred only at very low levels, they were not investigated further.

3.2. Development of multiple reaction monitoring (MRM) and selected reaction monitoring (SRM) targeted MS methods for the detection of 3-nitrotyrosine

It was difficult to detect nitration of fibrinogen in clinical samples by untargeted analysis, suggesting that the level of modification was lower than in fibrinogen nitrated *in vitro*.

Therefore, to improve the selectivity and sensitivity, an MRM analysis method was developed using data from fibrinogen nitrated *in vitro* to select specific tyrosine positions and determine the fragment ions to monitor. Nine tyrosine residues were selected for analysis: Y62, Y277 and Y589 from the α chain, Y71, Y408, Y452 and Y475 from the β chain, and Y380 and Y389 from the γ chain. This selection was made in order to include all the nitrated positions observed in the lowest nitration level plus two positions observed in the medium level of nitration, and two positions observed in the highest level of nitration. For each of those tyrosine residues, a native parent peptide (in its most common charge state) and the corresponding nitrated peptide were selected, prioritizing those showing higher intensity XIC peaks with suitable signal-to-noise ratios (> 8). Three transitions were selected with the aim of achieving correct identification based on specificity (only present in the parent ion of interest), intensity (higher signal to noise ratio) and including the tyrosine residue, for each one of the parent peptide ions. The collision energies (CE) for the peptides were calculated as CE = (slope) x (m/z + intercept), where slope and intercept were dependent on the peptide charge (2^+: 0.050 and 5, 3^+: 0.048 and -2, respectively). **Table 3** shows a list of the parent ions selected and the transitions with their masses, charges and collision energies.

The MRM methods were evaluated with fibrinogen nitrated *in vitro* (at the highest peroxynitrite ratio) and untreated fibrinogen. As expected, all the selected residues were found to be nitrated in nitrated fibrinogen and no nitrations were found in non-nitrated commercial fibrinogen (data not shown). A set of five clinical samples from each group were also analysed and gave encouraging results, but the analysis of the 9 nitration sites was very time consuming (only 3 nitration sites could be achieved in the 1 hour chromatographic run), so to increase the sensitivity and allow transitions for all 9 nitrated and native peptides to be analysed in a single chromatographic run, an SRM method was developed. The method used the same parent peptide *m/z* but only the transition with the highest intensity. **Figure 2** shows the MRM (**A and B**) and SRM (**C and D**) ion chromatograms of the peptide β^{472}GSWYSMR^{478} in its nitrated and

native forms, as an example. The peptide retention times obtained in the MRM experiments shifted (approx. half a minute) in the SRM experiments, but the distances between the modified and unmodified pairs were the very similar.

3.3. Analysis of clinical samples using the SRM method

The SRM method developed was applied to analyze enriched fibrinogen from plasma samples belonging to two clinical groups: ischemic stroke patients and non-inflammatory control patients. For each sample, the percentages of 3-nitrotyrosine were calculated for each of the selected tyrosine positions detected. Both clinical groups were compared statistically to search for significant differences between groups in any of the 3-nitrotyrosine residues detected. A Kolmogorov Smirnov test rejected Gaussian distribution of the resulting data, and a Mann-Whitney U test was then used to compare the two clinical groups between them. **Figure 3** shows the boxplots for each tyrosine residue analyzed, comparing ischemic stroke and non-inflammatory control groups. The plots show the mean, median, outliers, minimum and maximum value, as well as first and third quartile of the percentage of nitration. For clarity, some points are not shown on the plot, but these data values were used in the statistical calculations. Significant differences between groups and the corresponding p values from the Mann-Whitney U test are indicated.

Comparing the ischemic stroke and non-inflammatory control groups, a significant difference was found for three specific tyrosine residues: β452, β475 and γY380. For tyrosine residues β452 and β475 the percentages of nitrotyrosine observed for samples from the non-inflammatory control group were very low, similar to those observed for the unmodified fibrinogen samples described in Section 3.1. Even though some nitration was observed at residue γ380 in samples from the clinical control group, a significantly higher level was demonstrated in the ischemic stroke group. Tyrosine residues α62, α589 and γ389 showed no differences between ischemic stroke and control groups, with similar nitration levels to untreated fibrinogen samples. For residues α62 and γ389 the nitration levels were low, except

for a few samples (outliers shown in Figure 3). For tyrosine residue α589 and βY408 there was a high background, which probably indicates matrix interference. The red arrows indicate which data points correspond to samples from smokers in the ischemic stroke cohort, and it can be seen that they appear quite randomly distributed within the dataset.

In order to explore any potential association between the 3-nitrotyrosine residues detected and the condition of ischemic stroke, receiver-operating characteristics (ROC) curves were generated, to assess the capacity for each 3-nitrotyrosine position to predict ischemic stroke, individually and in different combinations. **Table 4** shows the areas under the curves (AUC). The occurrence of 3-nitrotyrosine at the position β452 showed the best association with the disease with the greatest AUC of 0.920 (95 % CI: 0.807 to 1.034). In contrast, no association was observed for residues α62, β71, β408 and γ389. Furthermore, association between ischemic stroke and different combinations of 3-nitrotyrosine positions were investigated. The best results were observed when β452, β475 and γ380 were combined, with an AUC of 0.896 (95 % CI: 0.790 to 1.002), which was slightly higher than the AUC achieved when γ380 either with β452 or β475 were combined, as shown in **Figure 4**.

Additionally, the pattern of nitration of the selected tyrosine residues was compared for nitration *in vivo* (ischemic stroke and non-inflammatory conditions), fibrinogen from plasma nitrated *ex vivo* and fibrinogen nitrated *in vitro*. **Figure 5** shows a plot of the distribution of nitration between tyrosine residues as a percentage of the total nitration in each sample type, and it can be seen that the profiles of the patient samples were similar, but different to the profiles of samples treated with peroxynitrite *in vitro* or *ex vivo*. The tyrosine residue contributing most to fibrinogen nitration *in vivo* was γY380, which corresponded to nearly half of the total nitration, followed by βY408, which contributed 16-27 %. In contrast, in fibrinogen nitrated in vitro using peroxynitrite there was a much more homogeneous distribution of nitration among the nine residues, with no single tyrosine contributing more than 20 %. The profile differed slightly between fibrinogen treated *in vitro*, where the three tyrosines in the α

chain, residue βY71 and residue γY389 were the most nitrated ones, and plasma nitrated *ex vivo*, in which residues αY589 and γY389 were the most nitrated ones. It is important to bear in mind that the total levels of nitrotyrosine were not the same in all four samples, so no direct comparison can be made for the amounts of nitrotyrosine at specific sites, only differences in distribution of nitration.

4. Discussion

Although peroxynitrite production and nitrotyrosine formation are thought to occur in ischemic stroke [29], as yet no studies have investigated nitration of specific fibrinogen tyrosine residues in this condition or their value as a diagnostic marker. Therefore, in this study we first mapped the sites of nitrotyrosine formation in fibrinogen treated with peroxynitrite *in vitro* using LC-MS/MS, and showed that at a molar ratio of 200:1 $ONOO^-$: fibrinogen, 20 out of the 49 tyrosine residues observed were modified. In terms of number of sites modified and % nitrotyrosine per peptide, was generally lower with the lower treatment ratios. The analysis identified 7 tyrosine nitration sites that we believe have not been reported previously: αY62, αY222, βY315, βY375, γY288, γY375 and γY380. We then developed a targeted method for detecting nitration of the most susceptible residues by single reaction monitoring (SRM), and applied this to fibrinogen enriched from plasma samples from patients with ischemic stroke, or from patients with non-inflammatory conditions as assessed by low levels of CRP. By this method we were able to provide the first evidence to demonstrate that the % nitration of tyrosine in fibrinogen is increased in the first 36 hours of ischemic stroke, compared to non-ischemic and non-inflammatory emergency conditions, and that nitration of specific residues or combinations of residues may have potential as a diagnostic tool. A proviso is that the ischemic disease and control patient groups were not perfectly matched, which is discussed further below. The analysis of fibrinogen nitration *in vitro* and comparison with nitration under pathophysiological conditions provides some interesting scientific insights.

The mapping of tyrosine nitration in fibrinogen treated *in vitro* was carried out using a un-targeted LC-MS/MS, which the peroxynitrite concentration-dependent susceptibility of the different chains and of residues therein to tyrosine nitration to be investigated. As far as we can ascertain, this is the first study to quantify as % modification the level of nitration in specific fibrinogen peptides using peptide XICs from an information-dependent LC-MS/MS approach. Concentration dependence of human fibrinogen nitration by peroxynitrite at molar ratios of 1.7:1 to 170:1 has previously been reported by Nowak *et al.* [35], using western blotting with anti-nitrotyrosine polyclonal antibodies, and they also observed high susceptibility of the alpha chain tyrosine residues to modification. Three previous studies used LC-MS/MS to investigate fibrinogen nitration. Meredith *et al.* reported that Y277 in the α chain (tryptic peptide ^{272}GGSTSY^{+45}GTGSETESPR^{287}) and Y135 in the γ chain (^{135}Y^{+45}LQEIYNSNNQK^{146}) were the tyrosine residues most susceptible to nitration by SIN-1 (a peroxynitrite generator), although no % nitration values were reported [36]. Residue αY277 was also the most highly modified in our study, but γY135 was modestly nitrated at 14% for the highest treatment. Luo *et al.* identified 15 nitrotyrosine sites in the γ chain of which Y96, Y262, Y274, Y348, and Y363 were most susceptible, but did not quantify the extent of modification at specific residues (Luo et al. 2015). Tang *et al.* used a peroxynitrite: fibrinogen molar ratio of ~330, and reported seven nitrated tyrosine residues in the α chain (two of them in the less common isoform), ten 3-nitrotyrosine sites in the β chain and nine in the γ chain, of which αY277, βY71, βY172, βY182, γY135 and γY389 were the most nitrated ones [33]. This study did not use primary MS signal intensity to calculate the extent of peptide nitration, but instead reported the number of MS/MS spectra identified for the nitrated or native peptides using the SEQUEST algorithm, apparently without de novo sequencing. This, as well as the higher ratio of peroxynitrite they used, may have contributed to larger number of nitrated positions reported compared to our findings. A third study used affinity capture of nitrated fibrinogen and its tryptic peptides to enrich nitrated peptides, which led to a focus on the beta chain, where 2 different residues, βY292 and βY422,

were consistently detected [22]. However, the use of peptide capture meant that % modification of these peptides could not be determined.

It is important to bear in mind that peroxynitrite can cause a variety of oxPTMs, including formation of hydroxytyrosine and as well as oxidation of methionine (to sulfoxide or sulfone), cysteine and tryptophan, as well as nitration of the latter [40-42]. The presence of multiple different oxPTMs, not only is significant in terms of overall damage but may also complicate the analysis by LC-MS/MS leading to potential false negatives if the modifications present are not included in the database searches [42]. To avoid this, we also used expanded oxPTM lists and error-tolerant searches, but other than methionine oxidation surprisingly few additional modifications were detected (no cysteine tri-oxidation, only 2 nitro-tryptophan containing peptides and one with oxidation of H or W), rarely on peptides containing nitrotyrosine. Therefore it is unlikely that such modifications would have affected significantly the accuracy of quantification. It is also known that the ionization efficiency determines how accurately peptides are identified and this can be affected by some PTMs, including nitrotyrosine [43, 44]. Finally, a proviso in untargeted LC-MS/MS analysis is always that if sequence coverage is incomplete, no conclusions can be drawn on the occurrence of modifications in peptides outwith the coverage.

It is clear that sites of nitration in fibrinogen are highly dependent on small variations in treatment conditions, such as the molar ratio, source of peroxynitrite, or possibly the type of instrument and parameters used. Moreover, it is generally accepted that the presence of CO_2 enhances nitrotyrosine formation by peroxynitrite, through reaction via the peroxynitrosocarbonate anion to form carbonate radical and nitrogen dioxide [13]. As our fibrinogen treatments in vitro were carried out in bicarbonate buffer, formation of the peroxynitrosocarbonate anion was likely and could have enhanced nitrotyrosine formation, as reported previously for glutamine synthetase [11], Mn SOD [45], surfactant protein A [46], bovine serum albumin and plasma [10]). It appears that the effects of carbon dioxide may be protein-dependent and complex. For the extracellular matrix protein laminin the presence of

bicarbonate reduced peroxynitrite-induced laminin aggregation on SDS PAGE [47]. More detailed analysis by LC-MS/MS suggested that tryptophan nitration was inhibited by CO_2, whereas dinitration of tyrosine was enhanced even at molar excesses of 5-500-fold [48]. This may explain the very low incidence of nitro-tryptophan observed in our fibrinogen samples treated in vitro. Bicarbonate has also been reported to inhibit methionine sulfoxide formation [11], thus altering the balance of oxPTMs; we observed oxidation of methionines in all samples (both in vitro and clinical), but as no experiments were carried out in the absence of CO_2 we cannot comment on its effect.

Although tyrosine nitration could be detected at lowest peroxynitrite treatment ratio, no 3-nitrotyrosine was detected in fibrinogen from clinical samples by the untargeted approach, which probably reflects the low % modification present. To address this limitation, other authors employed a capture step with antibodies against 3-nitrotyrosine [22, 49, 50], or cation-exchange HPLC [51] for the enrichment of nitrated proteins or nitrated peptides before LC-MS/MS analysis but, as mentioned above, this can introduce bias in the analysis. In contrast, we used a targeted MSMS analysis to improve sensitivity, including transitions to detect modifications observed in the lowest peroxynitrite treatment (Y62 from the α chain, Y71, Y408 and Y475 from β chain, and Y389 from γ chain) as well as several others there were consistently nitrated (277 and Y589 from α chain, Y452 from β chain and Y380 from γ chain). This SRM method allowed detection of 3-nitrotyrosine residues in peroxynitrite-treated fibrinogen samples and in clinical samples, but not in the untreated fibrinogen samples. For three of the tyrosine residues analyzed (Y452 and Y475 in the β chain and Y380 in the γ chain), a statistically significant higher relative level of nitration was observed in nitrated fibrinogen from ischemic stroke patients' plasma compared to plasma from patients with non-inflammatory conditions. It is interesting that the ischemic stroke group contained some samples with high % nitration for most of the tyrosine residues analyzed; although they appeared as outliers and were not statistically relevant, they may reflect a sub-set of more severely affected patients that could be further explored in a larger sample

set. The ROC curve analysis clearly suggested an association between nitration of specific tyrosine residues (βY452; βY452 + βY475 + γY380; βY452 + γY380; βY475 + γY380) and the ischemic stroke cohort. This would support the hypothesis that fibrinogen is a target for nitration during ischemic stroke, and fits with previous findings that nitration of fibrinogen affects fibrin polymerization, clot architecture and physical properties both *in vitro* [17] and *in vivo* [22].

An important difference of our study from most others investigating nitroxidative stress-related pathologies, including the demonstration by immunoassay of increased nitrated fibrinogen in plasma of ischemic stroke patients [29], is that we used patients with non-inflammatory pathological conditions as our control cohort. This is important, as comparison with a healthy volunteer cohort is likely to lead to overemphasis of the differences; moreover, it does not provide information on the diagnostic value of a marker for a specific disease, as opposed to a general disease state. The fact that our control cohort is not a healthy group may explain at least partly why 3-nitrotyrosine at βY408 showed more scattered values compared to the ischemic stroke disease group. The level of nitration in clinical samples could be highly dependent on the time between the ischemic event and the blood sampling, so it is interesting that differences were observed at a relatively early stage (1 to 36 hours after the first symptoms), which is the period when differential diagnosis would be most useful. On the other hand, owing to the use of patients with non-inflammatory conditions, it was difficult to match perfectly some parameters; specifically, age, smoking and alcohol intake are not very well-matched. These confounding factors could have contributed to the differences in nitrotyrosine levels, although there was no evidence that fibrinogen from smokers within the ischemic stroke cohort clustered at high levels of nitrotyrosine. Nevertheless, it is not possible to state conclusively an association between the nitrotyorine levels and ischemic stroke.

While the data discussed above show that the tyrosine residues selected for analysis were useful indicators of nitration in ischemic stroke patients, we discovered that the profile of residue nitration (the % contribution of specific residues to the total fibrinogen nitration) was rather

different for fibrinogen nitrated *in vitro* or *ex vivo*. In particular, a few specific nitrotyrosine residues (γY380, βY408 and αY589) predominated *in vivo*, whereas the distribution of nitration *in vitro* was more homogenous. There are several possible reasons why the nitration profile may be different. As mentioned above, the fibrinogen and plasma treatments *in vitro* used bicarbonate buffer, which leads to formation of the peroxynitrosocarbonate anion and alters the profile of oxPTMs. This concentration of bicarbonate is considered to generate physiological levels of CO_2 [48], and therefore should not per se explain differences to clinical samples. Nevertheless, it would be of interest to perform i*n vitro* experiments without CO_2 to determine if it does result in a nitration profile to similar to *in vivo* findings. Alternatively, *in vivo*, different agents could be responsible for nitration, such as peroxynitrous acid (ONOOH) and heme peroxidases; moreover the protein concentration is higher and other proteins may compete for nitration. The dominant modifications *in vivo* were ones that gave high % modification in vitro, suggesting they are more susceptible. Another possible cause of differential nitration pattern is that a continuous low dose formation of nitrating agents may have a different action to bolus treatment, and the local environment (pH, antioxidants, competition by other targets) as well as the conformational state of the protein are also likely to influence nitration selectivity. Whatever the underlying reason, this illustrates the difficulty of reproducing the physiological nitroxidative environment *in vitro* and points to the need for caution when extrapolating data obtained *in vitro* to pathological situations, including for analytical design. Thus, a potential limitation of this study is that the targeted MS/MS method was based on tyrosine residues observed to be nitrated *in vitro*; while these demonstrated significant differences in ischemic stroke, it is possible that other residues might have been more extensively modified or have had more discriminatory power.

The location of nitrotyrosine in fibrinogen has also been analysed in other pathological conditions. Parastatidis *et al.* performed a LC-MS/MS analysis of nitrated fibrinogen from smokers and non-smokers; the immuno-enrichment step for nitrated peptides resulted in

peptides mainly from the β chain being detected, with βY322 and βY452 reported as the principal nitration sites [22]. Interestingly, while nitrated βY452 was an important predictor of ischemic stroke in our study, it was not very highly nitrated *in vivo*. We also observed a peptide containing βY322 in untargeted analysis of peroxynitrite-treated fibrinogen, but the site of nitration was βY315. This difference may reflect the distinct methodological approach, or the different pathology of the cohort studied. Another study using immuno-precipitation reported that the fibrinogen β chain tended to present positive reactivity to polyclonal anti-nitrotyrosine antibodies in acute respiratory distress syndrome patients [25]. These findings may be explained by the fact that the beta chain contains more tyrosine residues than the other two chains so there are more possible sites of nitration, but it also supports our observation that two of the three tyrosine residues with highest % nitration in ischemic stroke were from the β chain. The analysis of plasma nitration targets in chronic end-stage kidney disease, a condition exhibiting high levels of inflammation and nitroxidative stress, found all three chains of fibrinogen were nitrated along with a number of other plasma proteins, but did not map the locations of the nitrotyrosine residues [27].

5. Conclusion

This work represents the first study to investigate the occurrence of nitrated fibrinogen in early stages of ischemic stroke, and to use a targeted LC-MS/MS approach to show increased nitration of specific tyrosine residues in an ischemic stroke cohort compared to one with non-inflammatory pathology. The data suggest that nitrated fibrinogen may be a potential biomarker of acute ischemic processes that might help with an earlier, specific diagnosis of ischemic stroke, but further work with a larger sample set and a better matched non-inflammatory disease cohort including smokers should be carried out to confirm this and explore the diagnostic value of additional nitrotyrosine locations. The different profiles of tyrosine nitration observed emphasize the potential of nitrotyrosine mapping to distinguish different experimental,

physiological or pathological conditions, but also point out the need for caution in extrapolating from results *in vitro*, as well as for standards of nitrated fibrinogen that more closely resemble physiological circumstances. For absolute quantification of specific nitrotyrosines, isotopically labeled nitrated and native peptides would be required. Despite the huge challenge of quantifying specific 3-nitrotyrosine residues, more disease-specific tools could ultimately reduce the mortality, neurological deficits and systemic damage associated with late diagnosis [6].

Funding/acknowledgements

This project has received funding from Comisión Sectorial de Investigación Científica (CSIC), from PEDECIBA-QUÍMICA, and from the European Union's Horizon 2020 research and innovation programme under the Marie Sklowdowska-Curie grant agreement number 675132 www.masstrplan.org. Experimental data will be available online at Aston Research Data Explorer (http://researchdata.aston.ac.uk/id/eprint/493/).

Author contributions

RM designed the study, prepared samples, analysed all data, drafted manuscript. BS assisted in MS data acquisition & analysis. SR sample collection and corrected the manuscript. CA assisted in MS data acquisition. LB sample collection and data analysis. ARP directed MS analysis, analysed MS data, corrected the manuscript. EL designed the study, corrected the manuscript. CMS helped design and manage the study, corrected the manuscript. GB designed the study, commented on the manuscript.

Abbreviations

CAD, Coronary artery disease; CID, Collision induced dissociation; COPD, Chronic obstructive pulmonary disease; CTL, Non-inflammatory condition control; ESI, Electrospray ionization; Fg,

Fibrinogen; hsCRP, high sensitivity C-Reactive protein; IDA, Information dependent acquisition; IS, Ischemic stroke; LC-MS/MS, Liquid chromatography-mass spectrometry; LDL, Low density lipoprotein; MI, Myocardial infarction; MRM, Multiple reaction monitoring; MS/MS, Tandem mass spectrometry; NC, Negative control; NIT PLASMA, *In vitro* nitrated plasma; oxPTM, Oxidative post translational modification; PBS, Phosphate-buffered saline; PC, Positive control; PEG, Polyethylene glycol; QTOF, Quadrupole time of flight; rtPA, recombinant tissue plasminogen activator; SIN-1, 3-morpholinosydnonimine; SRM, Selected reaction monitoring; XIC, Extracted ion chromatogram.

REFERENCES

[1] V.L. Feigin, C.M. Lawes, D.A. Bennett, S.L. Barker-Collo, V. Parag, Worldwide stroke incidence and early case fatality reported in 56 population-based studies: a systematic review, Lancet Neurol 8(4) (2009) 355-69.

[2] T. Ingall, Stroke--incidence, mortality, morbidity and risk, J Insur Med 36(2) (2004) 143-52.

[3] T.D. Musuka, S.B. Wilton, M. Traboulsi, M.D. Hill, Diagnosis and management of acute ischemic stroke: speed is critical, CMAJ 187(12) (2015) 887-93.

[4] J.C. Chavez, O. Hurko, F.C. Barone, G.Z. Feuerstein, Pharmacologic interventions for stroke: looking beyond the thrombolysis time window into the penumbra with biomarkers, not a stopwatch, Stroke 40(10) (2009) e558-63.

[5] W. Hacke, M. Kaste, E. Bluhmki, M. Brozman, A. Davalos, D. Guidetti, V. Larrue, K.R. Lees, Z. Medeghri, T. Machnig, D. Schneider, R. von Kummer, N. Wahlgren, D. Toni, E. Investigators, Thrombolysis with alteplase 3 to 4.5 hours after acute ischemic stroke, N Engl J Med 359(13) (2008) 1317-29.

[6] D.T. Laskowitz, S.E. Kasner, J. Saver, K.S. Remmel, E.C. Jauch, B.S. Group, Clinical usefulness of a biomarker-based diagnostic test for acute stroke: the Biomarker Rapid Assessment in Ischemic Injury (BRAIN) study, Stroke 40(1) (2009) 77-85.

[7] F.X. Guix, I. Uribesalgo, M. Coma, F.J. Munoz, The physiology and pathophysiology of nitric oxide in the brain, Prog Neurobiol 76(2) (2005) 126-52.

[8] M.A. Moro, A. Cardenas, O. Hurtado, J.C. Leza, I. Lizasoain, Role of nitric oxide after brain ischaemia, Cell Calcium 36(3-4) (2004) 265-75.

[9] K. Niizuma, H. Endo, P.H. Chan, Oxidative stress and mitochondrial dysfunction as determinants of ischemic neuronal death and survival, J Neurochem 109 Suppl 1 (2009) 133-8.

[10] A. Gow, D. Duran, S.R. Thom, H. Ischiropoulos, Carbon dioxide enhancement of peroxynitrite-mediated protein tyrosine nitration, Arch Biochem Biophys 333(1) (1996) 42-8.

[11] B.S. Berlett, R.L. Levine, E.R. Stadtman, Carbon dioxide stimulates peroxynitrite-mediated nitration of tyrosine residues and inhibits oxidation of methionine residues of glutamine synthetase: both modifications mimic effects of adenylylation, Proc Natl Acad Sci U S A 95(6) (1998) 2784-9.

[12] R. Radi, T.P. Cosgrove, J.S. Beckman, B.A. Freeman, Peroxynitrite-induced luminol chemiluminescence, Biochem J 290 (Pt 1) (1993) 51-7.

[13] G. Ferrer-Sueta, N. Campolo, M. Trujillo, S. Bartesaghi, S. Carballal, N. Romero, B. Alvarez, R. Radi, Biochemistry of Peroxynitrite and Protein Tyrosine Nitration, Chem Rev 118(3) (2018) 1338-1408.
[14] A. Abulrob, E. Brunette, J. Slinn, E. Baumann, D. Stanimirovic, In vivo optical imaging of ischemic blood-brain barrier disruption, Methods Mol Biol 763 (2011) 423-39.
[15] J.S. Beckman, T.W. Beckman, J. Chen, P.A. Marshall, B.A. Freeman, Apparent hydroxyl radical production by peroxynitrite: implications for endothelial injury from nitric oxide and superoxide, Proc Natl Acad Sci U S A 87(4) (1990) 1620-4.
[16] M. Tajes, G. Ill-Raga, E. Palomer, E. Ramos-Fernandez, F.X. Guix, M. Bosch-Morato, B. Guivernau, J. Jimenez-Conde, A. Ois, F. Perez-Asensio, M. Reyes-Navarro, C. Caballo, A.M. Galan, F. Alameda, G. Escolar, C. Opazo, A. Planas, J. Roquer, M.A. Valverde, F.J. Munoz, Nitro-oxidative stress after neuronal ischemia induces protein nitrotyrosination and cell death, Oxid Med Cell Longev 2013 (2013) 826143.
[17] M. Martinez, J.W. Weisel, H. Ischiropoulos, Functional impact of oxidative posttranslational modifications on fibrinogen and fibrin clots, Free Radic Biol Med 65 (2013) 411-418.
[18] M.W. Mosesson, Fibrinogen and fibrin structure and functions, J Thromb Haemost 3(8) (2005) 1894-904.
[19] M. Di Napoli, P. Singh, Is plasma fibrinogen useful in evaluating ischemic stroke patients?: why, how, and when, Stroke 40(5) (2009) 1549-52.
[20] E. Shacter, J.A. Williams, R.L. Levine, Oxidative modification of fibrinogen inhibits thrombin-catalyzed clot formation, Free Radic Biol Med 18(4) (1995) 815-21.
[21] J. Kanski, A. Behring, J. Pelling, C. Schoneich, Proteomic identification of 3-nitrotyrosine-containing rat cardiac proteins: effects of biological aging, Am J Physiol Heart Circ Physiol 288(1) (2005) H371-81.
[22] I. Parastatidis, L. Thomson, A. Burke, I. Chernysh, C. Nagaswami, J. Visser, S. Stamer, D.C. Liebler, G. Koliakos, H.F. Heijnen, G.A. Fitzgerald, J.W. Weisel, H. Ischiropoulos, Fibrinogen beta-chain tyrosine nitration is a prothrombotic risk factor, J Biol Chem 283(49) (2008) 33846-53.
[23] B. Lipinski, Pathophysiology of oxidative stress in diabetes mellitus, J Diabetes Complications 15(4) (2001) 203-10.
[24] C. Vadseth, J.M. Souza, L. Thomson, A. Seagraves, C. Nagaswami, T. Scheiner, J. Torbet, G. Vilaire, J.S. Bennett, J.C. Murciano, V. Muzykantov, M.S. Penn, S.L. Hazen, J.W. Weisel, H. Ischiropoulos, Pro-thrombotic state induced by post-translational modification of fibrinogen by reactive nitrogen species, J Biol Chem 279(10) (2004) 8820-6.
[25] M.D. Gole, J.M. Souza, I. Choi, C. Hertkorn, S. Malcolm, R.F. Foust, 3rd, B. Finkel, P.N. Lanken, H. Ischiropoulos, Plasma proteins modified by tyrosine nitration in acute respiratory distress syndrome, Am J Physiol Lung Cell Mol Physiol 278(5) (2000) L961-7.
[26] B. Pignatelli, C.Q. Li, P. Boffetta, Q. Chen, W. Ahrens, F. Nyberg, A. Mukeria, I. Bruske-Hohlfeld, C. Fortes, V. Constantinescu, H. Ischiropoulos, H. Ohshima, Nitrated and oxidized plasma proteins in smokers and lung cancer patients, Cancer Res 61(2) (2001) 778-84.
[27] M. Piroddi, A. Palmese, F. Pilolli, A. Amoresano, P. Pucci, C. Ronco, F. Galli, Plasma nitroproteome of kidney disease patients, Amino Acids 40(2) (2011) 653-67.
[28] M. Martinez, A. Cuker, A. Mills, R. Lightfoot, Y. Fan, W.H. Tang, S.L. Hazen, H. Ischiropoulos, Nitrated fibrinogen is a biomarker of oxidative stress in venous thromboembolism, Free Radic Biol Med 53(2) (2012) 230-6.
[29] G. Ill-Raga, E. Palomer, E. Ramos-Fernandez, F.X. Guix, M. Bosch-Morato, B. Guivernau, M. Tajes, V. Valls-Comamala, J. Jimenez-Conde, A. Ois, F. Perez-Asensio, M. Reyes-Navarro, C. Caballo, G. Gil-Gomez, I. Lopez-Vilchez, A.M. Galan, F. Alameda, G. Escolar, C. Opazo, A.M. Planas, J. Roquer, M.A. Valverde, F.J. Munoz, Fibrinogen nitrotyrosination after ischemic stroke impairs thrombolysis and promotes neuronal death, Biochim Biophys Acta 1852(3) (2015) 421-8.
[30] J.M. Kollman, L. Pandi, M.R. Sawaya, M. Riley, R.F. Doolittle, Crystal structure of human fibrinogen, Biochemistry 48(18) (2009) 3877-86.

[31] G. Grieninger, X. Lu, Y. Cao, Y. Fu, B.J. Kudryk, D.K. Galanakis, K.M. Hertzberg, Fib420, the novel fibrinogen subclass: newborn levels are higher than adult, Blood 90(7) (1997) 2609-14.
[32] R.F. Doolittle, S. Hong, D. Wilcox, Evolution of the fibrinogen gamma' chain: implications for the binding of factor XIII, thrombin and platelets, J Thromb Haemost 7(8) (2009) 1431-3.
[33] Z. Tang, H. Wu, D. Du, J. Wang, H. Wang, W.J. Qian, D.J. Bigelow, J.G. Pounds, R.D. Smith, Y. Lin, Sensitive immunoassays of nitrated fibrinogen in human biofluids, Talanta 81(4-5) (2010) 1662-9.
[34] Y. Luo, J. Shi, J. Li, Peroxynitrite induced fibrinogen site identification, Biomed Mater Eng 26 Suppl 1 (2015) S2241-8.
[35] P. Nowak, H.M. Zbikowska, M. Ponczek, J. Kolodziejczyk, B. Wachowicz, Different vulnerability of fibrinogen subunits to oxidative/nitrative modifications induced by peroxynitrite: functional consequences, Thromb Res 121(2) (2007) 163-74.
[36] S. Meredith, G. Parekh, J. Towler, J. Schouten, P. Davis, H. Griffiths, C. Spickett, Mapping nitro-tyrosine modifications in fibrinogen by mass spectrometry as a biomarker for inflammatory disease, Free Radic Biol Med 75 Suppl 1 (2014) S50.
[37] M.O. Longas, J. Newman, A.J. Johnson, An improved method for the purification of human fibrinogen, Int J Biochem 11(6) (1980) 559-64.
[38] J.S. Beckman, J. Chen, H. Ischiropoulos, J.P. Crow, Oxidative chemistry of peroxynitrite, Methods Enzymol 233 (1994) 229-40.
[39] P.M. Ridker, Cardiology Patient Page. C-reactive protein: a simple test to help predict risk of heart attack and stroke, Circulation 108(12) (2003) e81-5.
[40] C. Houee-Levin, K. Bobrowski, L. Horakova, B. Karademir, C. Schoneich, M.J. Davies, C.M. Spickett, Exploring oxidative modifications of tyrosine: an update on mechanisms of formation, advances in analysis and biological consequences, Free Radic Res 49(4) (2015) 347-73.
[41] R. Radi, Oxygen radicals, nitric oxide, and peroxynitrite: Redox pathways in molecular medicine, Proc Natl Acad Sci U S A 115(23) (2018) 5839-5848.
[42] I. Verrastro, S. Pasha, K.T. Jensen, A.R. Pitt, C.M. Spickett, Mass spectrometry-based methods for identifying oxidized proteins in disease: advances and challenges, Biomolecules 5(2) (2015) 378-411.
[43] L. Rezende Valim, J.A. Davies, K. Tveen Jensen, R. Guo, K.R. Willison, C.M. Spickett, A.R. Pitt, D.R. Klug, Identification and relative quantification of tyrosine nitration in a model peptide using two-dimensional infrared spectroscopy, J Phys Chem B 118(45) (2014) 12855-64.
[44] E.S. Witze, W.M. Old, K.A. Resing, N.G. Ahn, Mapping protein post-translational modifications with mass spectrometry, Nat Methods 4(10) (2007) 798-806.
[45] N.B. Surmeli, N.K. Litterman, A.F. Miller, J.T. Groves, Peroxynitrite mediates active site tyrosine nitration in manganese superoxide dismutase. Evidence of a role for the carbonate radical anion, J Am Chem Soc 132(48) (2010) 17174-85.
[46] S. Zhu, K.F. Basiouny, J.P. Crow, S. Matalon, Carbon dioxide enhances nitration of surfactant protein A by activated alveolar macrophages, Am J Physiol Lung Cell Mol Physiol 278(5) (2000) L1025-31.
[47] G. Degendorfer, C.Y. Chuang, A. Hammer, E. Malle, M.J. Davies, Peroxynitrous acid induces structural and functional modifications to basement membranes and its key component, laminin, Free Radic Biol Med 89 (2015) 721-33.
[48] L.G. Lorentzen, C.Y. Chuang, A. Rogowska-Wrzesinska, M.J. Davies, Identification and quantification of sites of nitration and oxidation in the key matrix protein laminin and the structural consequences of these modifications, Redox Biol 24 (2019) 101226.
[49] M. Aslan, T.M. Ryan, T.M. Townes, L. Coward, M.C. Kirk, S. Barnes, C.B. Alexander, S.S. Rosenfeld, B.A. Freeman, Nitric oxide-dependent generation of reactive species in sickle cell disease. Actin tyrosine induces defective cytoskeletal polymerization, J Biol Chem 278(6) (2003) 4194-204.

[50] B.A. Petre, M. Ulrich, M. Stumbaum, B. Bernevic, A. Moise, G. Doring, M. Przybylski, When is mass spectrometry combined with affinity approaches essential? A case study of tyrosine nitration in proteins, J Am Soc Mass Spectrom 23(11) (2012) 1831-40.
[51] C. Batthyany, J.M. Souza, R. Duran, A. Cassina, C. Cervenansky, R. Radi, Time course and site(s) of cytochrome c tyrosine nitration by peroxynitrite, Biochemistry 44(22) (2005) 8038-46.

TABLES

Table 1. Characteristics of the patient populations

	Ischemic stroke (n=24)	**Non-inflammatory control (n=12)**
Age (mean and range in years)	70 (44 – 93)	49 (17 – 85) *
Gender (F/M)	12/12	8/4
Disease history and risk factors		
CAD/MI/angina	6	0
Stroke	10	0
COPD	3	0
Diabetes Mellitus	8	0
Arterial Hypertension	17	0
Hyperlipidemia	10	0
hsCRP (mg/L) (mean, range)	27.1 (0.4 – 273.1)	0.7 (0.1 – 1.0) *
Tobacco use	8	0
Alcohol use	7	0

CAD: Coronary Artery Disease; MI: Myocardial Infarction; COPD: Chronic Obstructive Pulmonary Disease; hsCRP: high sensitivity C-Reactive Protein

* $p < 0.05$

1 **Table 2. Fibrinogen (Fg) peptides identified to contain nitrotyrosine, grouped by fibrinogen polypeptide chain to show % nitration and 3 molar ratios of $ONOO^-$.**

Fg chain	Molar ratio $ONOO^-$/Fg 200	100	10	Tyrosine site	Identified modified peptide sequence [a]	Theoretical mass of modified peptide [b]	Observed mass of modified peptide [c]	m/z (charge state)	Ion score [d]	Rt [e] (min)
	% Tyrosine nitration [f]									
α	33	0	2	Y62	^{49}DSDWPFCSDEDWNY^{+45}K^{63}	2007.72	2007.87	670.23 (3+)	92	35.5
	55	0	0	Y95	^{88}LKNSLFE Y^{+45}QK^{97}	1313.66	1313.76	657.89 (2+)	55	24.5
	69	75	0	Y277	^{272}GGSTSY^{+45}GTGSETESPR^{287}	1616.66	1616.77	809.39 (2+)	83	19.2
	15	8	0	Y589	^{582}QFTSSTSY^{+45}NRGDSTFESK^{599}	2085.89	2086.05	696.36 (3+)	43	21.7
β	46	4	1	Y71	^{53}REEAPSLRPAPPPISGGG Y^{+45}R^{72}	2151.08	2151.25	718.09 (3+)	94	22.5
	16	-	0	Y149	^{125}NSVDELNNNVEAVSQTSSSSFQYMY^{+45}LLK^{152}	3211.46	3211.71	1071.58 (3+)	69	37.9
	2	0	0	Y172	^{164}DNENVVNEY^{+45}SSELEK^{178}	1812.77	1812.90	907.46 (2+)	61	29.8
	25	-	0	Y222	^{212}LESDVSAQMEY^{+45}CR^{224}	1631.66	1631.77	816.89 (2+)	79	28.6
	14	0	0	Y315	^{314}NY^{+45}CGLPGEYWLGNDK^{328}	1829.77	1829.91	915.96 (2+)	87	32.8
	21	0	0	Y375	^{354}AHYGGFTVQNEANKYQISVNKY^{+45}R^{376}	2731.31	2731.48	911.50 (3+)	131	25.0
	24	0	1	Y408	^{396}TMTIHNGMFFSTY^{+45}DR^{410}	1880.78	1880.92	627.98 (3+)	102	28.0
	1	0	0	Y447	^{446}YY^{+45}WGGQY^{+45}TWDMAK^{458}	1757.68	1757.82	879.91 (2+)	13	32.8
	9	0	0	Y452	^{446}YYWGGQY^{+45}TWDMAK^{458}	1712.69	1712.82	857.42 (2+)	71	32.3
	3	0	11	Y475	^{472}GSWY^{+45}SMR^{478}	930.37	930.42	466.22 (2+)	33	26.4
	14	0	0	Y135	^{135}Y^{+45}LQEIYNSNNQK^{146}	1557.71	1557.80	779.91 (2+)	41	23.3

	7	0	0	Y140	^{135}Y^{+45}LQEIY^{+45}NSNNQK^{146}	1602.69	1602.81	802.41 (2+)	37	26.5
	13	0	0	Y288	^{283}TSTADY^{+45}AMFK^{292}	1178.49	1178.57	590.29 (2+)	54	26.6
γ	23	0	0	Y375	^{365}CHAGHLNGVYY^{+45}QGGTY^{+45}SK^{382}	2100.87	2101.02	701.35 (3+)	74	22.0
	53	0	0	Y380	^{365}CHAGHLNGVYYQGGTY^{+45}SK^{382}	2055.89	2056.02	515.01 (4+)	68	20.8
	22	-	3	Y389	^{383}ASTPNGY^{+45}DNGIIWATWK^{399}	1937.89	1938.04	970.03 (2+)	108	34.1

[a] Superscript numbers indicate the position of the residue at the beginning and at the end of the sequence. The modified tyrosine residue is shown in red.
[b] The observed mass is calculated from the m/z of the ion observed in the mass spectrum
[c] the theoretical masses are calculated from the peptide sequence.
[d] the ion score is the average Mascot MOWSE score for the individual peptides
[e] Rt is the retention time of the peptide during chromatography.
[f] Relative quantification of nitrated peptide was calculated as a % of the total peptide of that sequence (nitrated + unmodified).
– indicates tyrosine position not covered.

1

1 **Table 3. Fibrinogen tryptic peptides selected for MRM analysis.**

Chain	Tyrosine position	Fibrinogen peptide sequence [a]	Parent ion m/z (charge state)	Product ion mass (fragment)	Collision Energy (volts)	Rt (min)
α	Y62	**^{49}DSDWPFCSDEDWNYK^{63}**	982.45 (2+)	**424.25 (y3)** [b] 610.35 (y4) 1216.57 (y9)	47.14	34.6
		^{49}DSDWPFCSDEDWNY^{+45}K^{63}	1004.95 (2+)	**318.12 (b3)** 655.34 (y4) 1101.51 (y8)	48.24	36.7
	Y277	**^{272}GGSTSYGTGSETESPR^{287}**	786.90 (2+)	862.45 (y8) **1020.54 (y10)** 1183.62 (y11)	37.56	18.3
		^{272}GGSTSY^{+45}GTGSETESPR^{287}	809.40 (2+)	862.45 (y8) **1020.54 (y10)** 1228.61 (y11)	38.66	20.8
	Y589	**^{582}QFTSSTSYNR^{591}**	595.81 (2+)	727.39 (y6) 814.43 (y7) **915.49 (y8)**	28.19	19.8
		^{582}QFTSSTSY^{+45}NR^{591}	618.31 (2+)	772.38 (y6) 859.42 (y7) **960.47 (y8)**	29.30	23.0
β	Y71	**^{54}EEAPSLRPAPPPISGGGYR^{72}**	651.05 (3+)	596.32 (y6) **806.48 (y8)** 903.54 (y9)	29.25	25.2
		^{54}EEAPSLRPAPPPISGGG Y^{+45}R^{72}	666.05 (3+)	641.31 (y6) **833.94 (y^{++}16)** 851.47 (y8)	29.97	27.0
	Y408	**^{396}TMTIHNGMFFSTYDR^{410}**	612.98 (3+)	554.30 (y4) **641.34 (y5)** 788.42 (y6)	27.42	29.8

		^{396}**TMTIHNGMFFSTY^{+45}DR^{410}**	627.98 (3+)	599.29 (y4) **686.33 (y5)** 833.41 (y6)	28.14	31.9
	Y452	^{446}**YYWGGQYTWDMAK^{458}**	556.95 (3+)	349.22 (y3) 464.25 (y4) **650.35 (y5)**	24.73	32.8
		^{446}**YYWGGQY^{+45}TWDMAK^{458}**	857.42 (2+)	959.48 (y7) 1144.60 (y9) **1201.60 (y10)**	41.01	33.7
	Y475	^{472}**GSWYSMR^{478}**	443.73 (2+)	393.22 (y3) **556.30 (y4)** 742.40 (y5)	20.74	26.2
		^{472}**GSWY^{+45}SMR^{478}**	466.22 (2+)	393.22 (y3) **601.29 (y4)** 787.38 (y5)	21.85	29.5
γ	Y380	^{365}**CHAGHLNGVYYQGGTYSK^{382}**	671.35 (3+)	**424.22 (b^{++}8)** 612.35 (y6) 1066.57 (y9)	30.23	21.7
		^{365}**CHAGHLNGVYYQGGTY^{+45}SK^{382}**	515.01 (4+)	424.22 (b++8) **657.34 (y6)** 946.50 (b9)	23.75	23.4
	Y389	^{383}**ASTPNGYDNGIIWATWK^{399}**	632.02 (3+)	505.32 (y4) 691.42 (y5) **804.51 (y6)**	28.34	33.9
		^{383}**ASTPNGY^{+45}DNGIIWATWK^{399}**	970.03 (2+)	434.27 (y3) 691.41 (y5) **840.47 (y^{++}14)**	46.53	35.7

[a] Superscript numbers correspond to the amino acid position in the mature protein for the start and end residues. Modified residues are shown in red.

[b] The corresponding product ions and the calculated collision energy are shown for modified and unmodified peptides. The transitions shown in bold were selected for the SRM method.

Table 2. Receiver operating characteristic (ROC) curve analysis for the 9 tyrosine residues analysed

Tyrosine position	ROC curve analysis	
	AUC [a]	95 % CI [b]
αY62	0.569	0.376 to 0.763
αY277	0.684	0.432 to 0.936
αY589	0.688	0.454 to 0.921
βY71	0.590	0.395 to 0.786
βY408	0.503	0.256 to 0.751
βY452	0.920	0.807 to 1.034
βY475	0.840	0.665 to 1.016
γY380	0.806	0.663 to 0.948
γY389	0.542	0.339 to 0.744
ALL	0.799	0.608 to 0.989
βY452-βY475-γY380	0.896	0.790 to 1.002
βY452-βY475	0.837	0.659 to 1.014
βY452-γY380	0.823	0.688 to 0.958
βY475-γY380	0.892	0.785 to 1.000

[a] area under the curve

[b] confidence interval

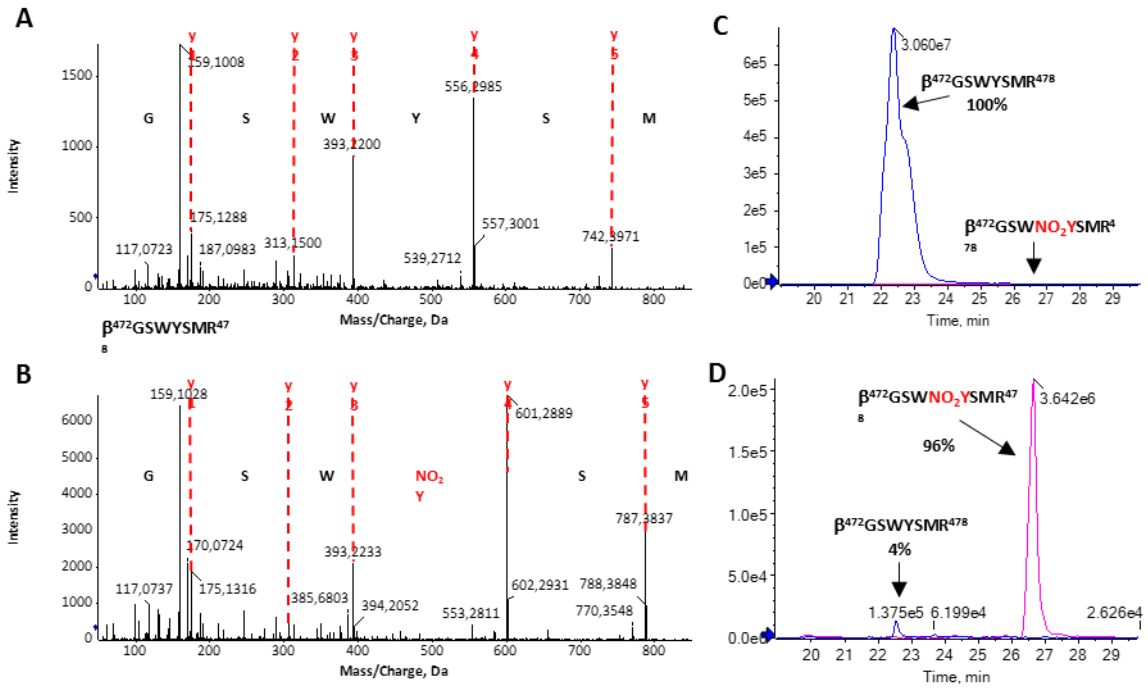

Figure 1. Identification of nitrotyrosine in the tryptic peptide βGSWYSMR of peroxynitrite-treated fibrinogen. MS/MS spectra of the tryptic peptide βGSWYSMR (**A**) and the corresponding nitrated peptide showing presence of nitrotyrosine (**B**) with the y ion series labelled. The mass shift from 556.30 Da to 601.29 Da supports the presence of a 3-nitrotyrosine modification at βY475. Corresponding extracted ion chromatograms of nitrated and unmodified forms of peptide βGSWYSMR used for relative quantification from control (untreated) fibrinogen (**C**) and peroxynitrite-treated fibrinogen (D). Representative data from biological triplicates.

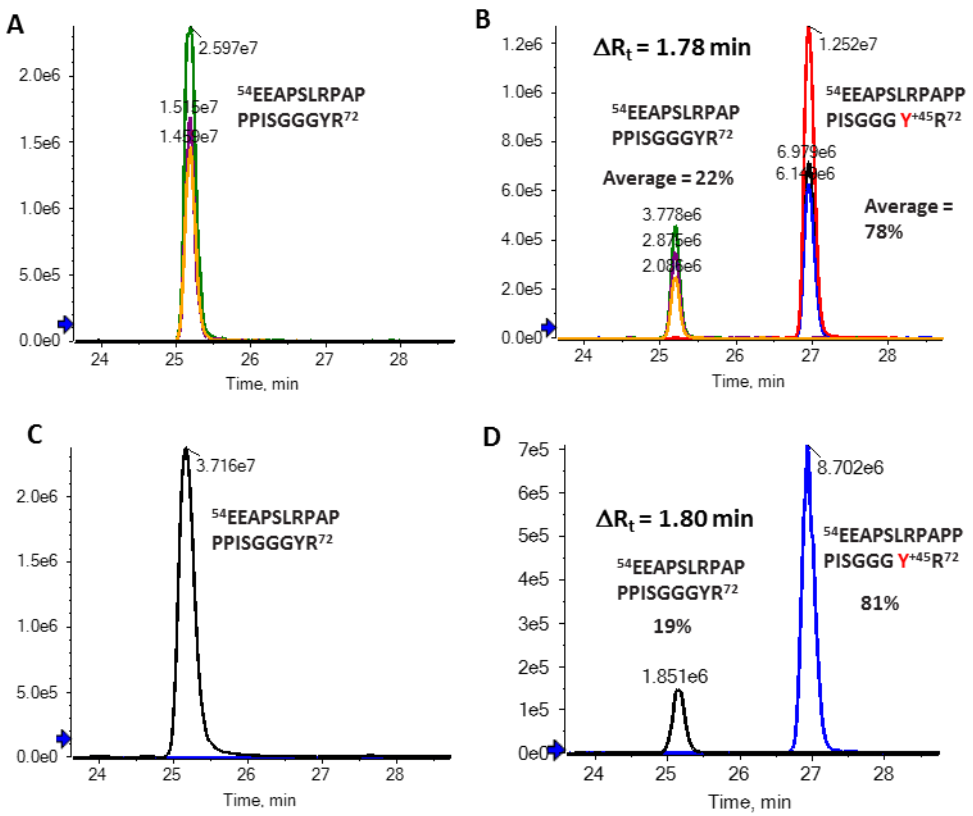

Figure 2. Comparison of targeted MSMS analysis of nitrated peptide β^{54}EEAPSLRPAPPPISGGGYR^{72} from fibrinogen nitrated in vitro. Extracted ion chromatograms of the peptide βEEAPSLRPAPPPISGGGYR containing the tyrosine residue 71 obtained by MRM analysis of the peptide from untreated (A) and modified (B) fibrinogen, and the corresponding SRMs of untreated (C) and modified (D) fibrinogen. The selected transitions, the peak areas, and the calculated relative percentage of each peptide are shown. A slight shift in absolute retention time was observed due to chromatographic variation between the experiments and the difference in the retention times between native and modified peptide are apparent. Representative data from biological triplicates.

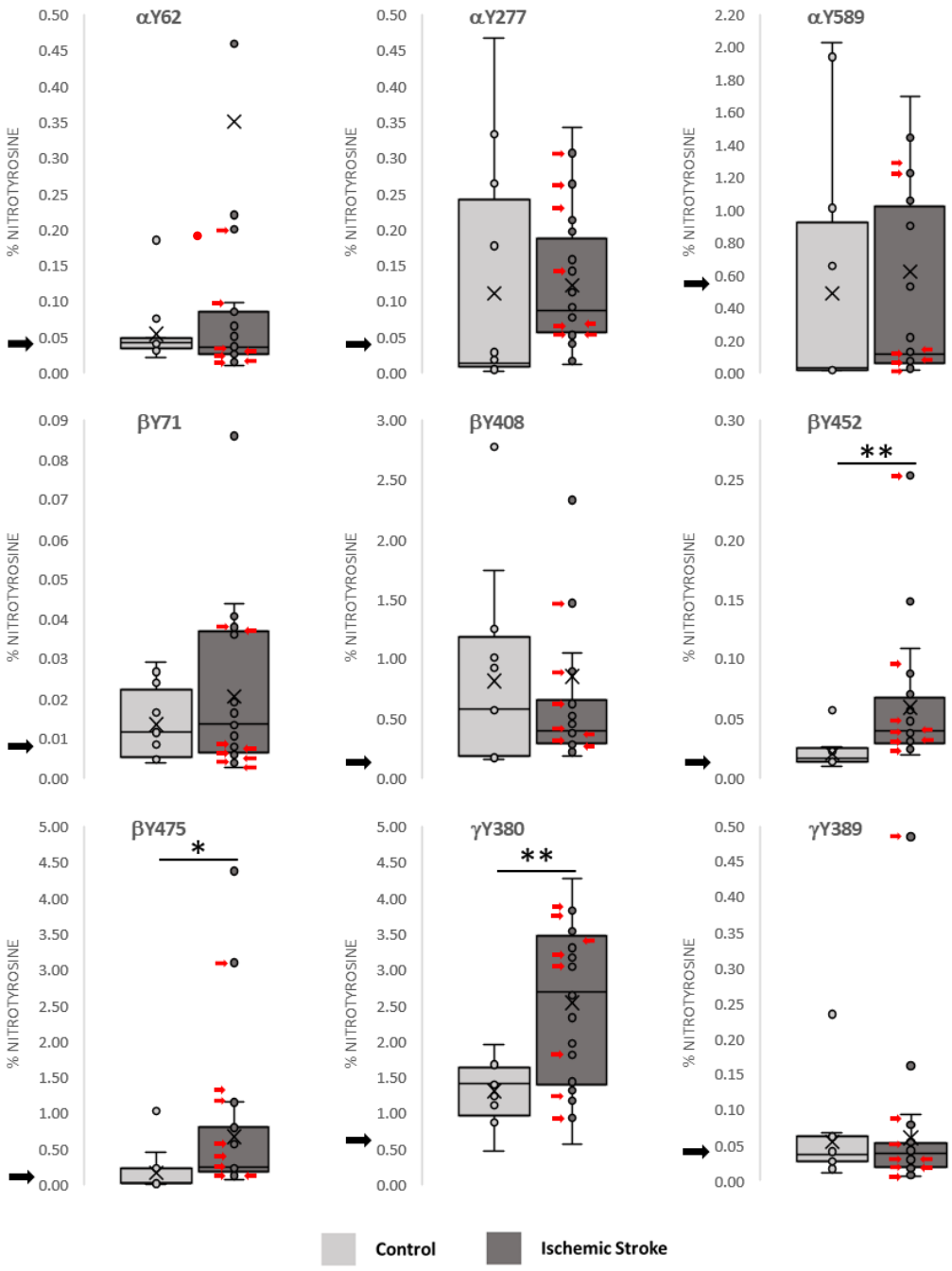

Figure 1. Boxplots of the percentage tyrosine nitration for each residue studied. The boxplots compare ischemic stroke patients (Ischemic Stroke) and non-inflammatory disease volunteers (Control) for all the tyrosine residues analysed. The source fibrinogen chain is indicated by a prefixed α, β or γ before the tyrosine residue number. P-values bands of the Mann-Whitney U tests for significant difference between groups are indicated by stars: * $p<0.003$, ** $p<0.001$. For clarity, three data points are not shown on the plots, all in the IS group (6.7 % in αY62, 5.4 % in αY589 and 7.5 % in βY408; smoker patients). The black arrows on the y-axes point to the mean value of the untreated fibrinogen. Red arrows show data from smoker patients. The central rectangle spans the first quartile to the third quartile (the interquartile range), a segment inside the rectangle shows the median, crosses show the mean and "whiskers" above and below the box show the locations of the minimum and maximum. Outliers were excluded in the figure for better presentation but included in the statistical analysis.

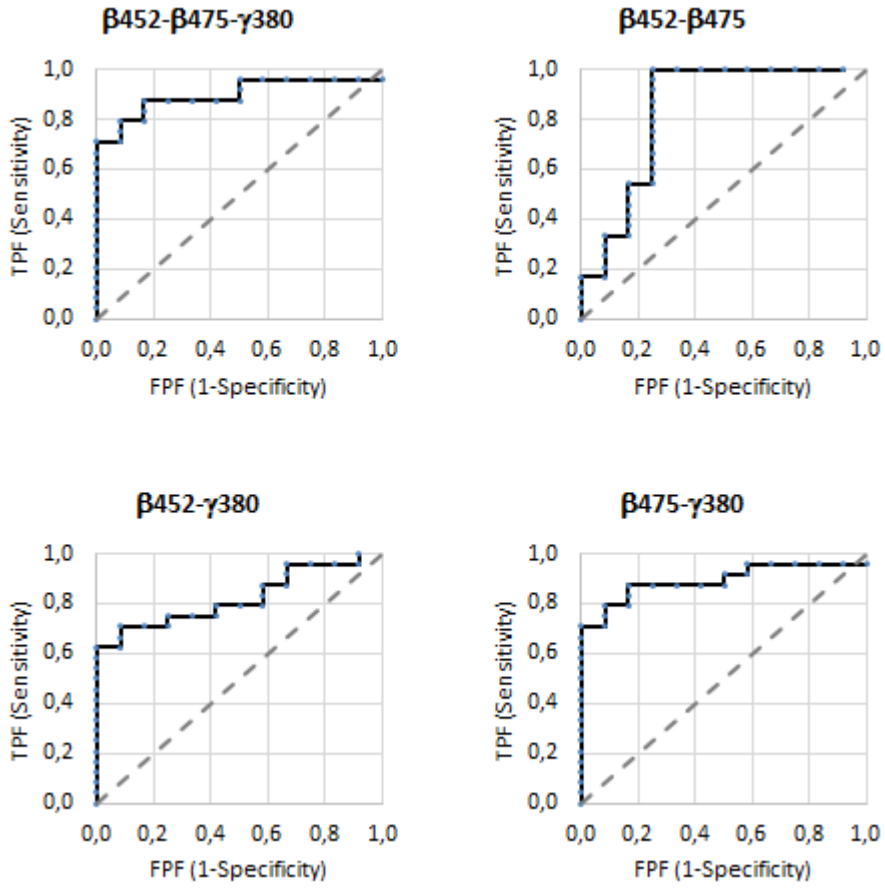

Figure 2. Receiver operating characteristic (ROC) curve analysis. Combinations of the most relevant modified tyrosine positions for prediction of ischemic stroke are shown.

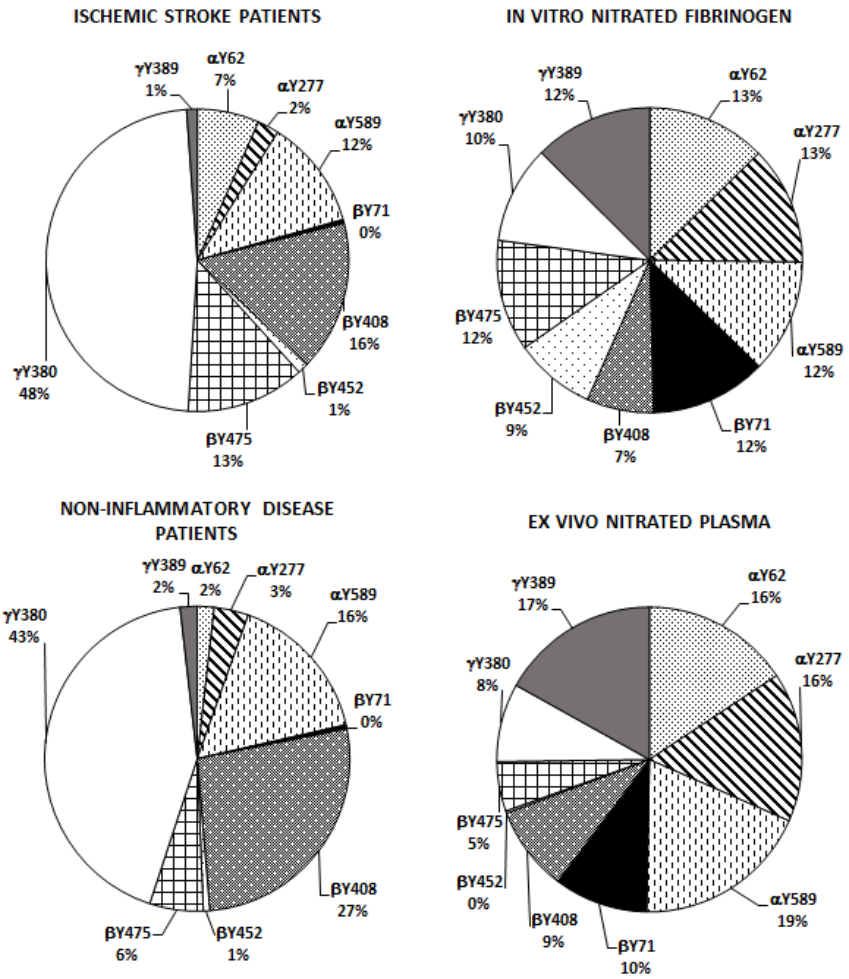

Figure 3. Percentage contribution to the total nitrotyrosine pool for the nine tyrosine residues analyzed. The nitrotyrosine profiles are shown for samples from ischemic stroke and non-inflammatory disease control groups and peroxynitrite-treated fibrinogen and plasma (nitration *in vitro* and *ex vivo*). It should be noted that the % nitration between sample sets cannot be compared absolutely as the total levels of nitration were not the same.

SUPPLEMENTARY INFORMATION

Supplementary Table S1. Theoretical tyrosine content, and observed tyrosine or nitrotyrosine content [1]

Treatment ratio (ONOOH: Fg)	**Nitrotyrosines Observed**	**Unmodified Tyrosines Observed**
Alpha Chain tyrosine content: α -1 isoform = 24Y (2% predominance); α-2 isoform = 9 Y (98% predominance)		
200:1	3	10 (9 from α-2)
100:1	2	6 (all from α-2)
10:1	1	10 (9 from α-2)
Untreated	0	13 (9 from α-2)
Beta Chain tyrosine content: 21 Y		
200:1	10	21
100:1	1	17
10:1	3	21
Untreated	0	21
Gamma Chain tyrosine content: ɣ-A isoform = 20 Y (predominant); ɣ-B isoform = 22 Y		
200:1	6	18
100:1	0	9
10:1	1	16
Untreated	0	15

[1] Data obtained from the information-dependent analysis experiments reported in Table 2.